Int. J. Electrochem. Sci., 11 **(2016)** 9614 – 9624, doi: 10.20964/2016.11.11

International Journal of ELECTROCHEMICAL SCIENCE
www.electrochemsci.org

Deposition of Au Nanoparticles onto Poly(3,4-ethylenedioxy - thiophene) Functionalized Multi-Walled Carbon Nanotubes for Label-Free Immunosensing

Li Min Lu[1], *Yan Sha Gao*[1,2], *Yin Xiu Zuo*[2], *Jing Kun Xu*[2,*], *Wen Min Wang*[1], *Haohua He* [1,*], *Ping Li*[1], *Yong Fang Yu*[1]

[1] College of Science, Jiangxi Agricultural University, Nanchang 330045, PR China
[2] Jiangxi Key Laboratory of Organic Chemistry, Jiangxi Science and Technology Normal University, Nanchang 330013, PR China
[*]E-mail: xujingkun@tsinghua.org.cn, hhhua64@163.com

Received: 15 July 2016 / *Accepted:* 29 August 2016 / *Published:* 10 October 2016

A high performance electrochemical immunosensor was constructed for sensitive label-free detection for α-fetoprotein (α-FP) based on Au nanoparticles/poly(3,4-ethylenedioxythiophene) modified multi-walled carbon nanotubes (AuNPs/PEDOT-MWCNTs), which acted as signal amplification matrix. PEDOT functionalized MWCNTs were prepared via interfacial polymerization method. PEDOT was uniformly distributed on MWCNTs, which can provide more binding sites for high mass loading of metal nanoparticles. Subsequently, AuNPs were attached on MWCNTs by introducing conductive PEDOT to bridge the AuNPs and MWCNTs walls. The AuNPs/PEDOT-MWCNTs nanocomposites displayed good electron transfer ability, which enabled good analytical properties for α-FP detection.

Keywords: Electrochemical method; Tumor marker; Poly(3,4-ethylenedioxythiophene) nanocomposites; High sensitivity

1. INTRODUCTION

In the past few years, it has been proven that electrode material and architecture play key roles in obtaining sensitive and stable detections in protein-based bioanalysis [1-2]. Multiwalled carbon nanotubes (MWCNTs) consisting of π-conjugated networks, possess large surface area, excellent thermal stability as well as high conductivity and are most exciting 1D nanomaterials due to their remarkable properties [3-7]. These excellent properties enable their use as attractive carrier for metal nanoparticles. Many methods have been used to attach metal nanoparticles onto MWCNTs, including electroless deposition [8], electrodeposition [9] and assembly strategy [10]. However, metal

nanoparticles fabricated in these fashions are unstable and easy to form agglomeration due to the inertness of MWCNTs walls. Usually, sol-gel and other binders such as polymer and surfactants have been employed for the decoration of CNT [11-14]. However, the preparation of sol-gel matrix must be completed under harsh operating conditions, and binders could increase the electron-transfer resistance. In contrast, conductive polymers should be ideal materials for surface decoration of MWCNTs owing to their excellent electrical and electrochemical properties. Moreover, the composites of conducting polymer/MWCNTs can perform special properties through the synergistic effect of conducting polymer and MWCNTs.

A-fetoprotein (α-FP) is a single-chain oncofetal glycoprotein with a molecular weight of approximately 70,000 Da. Usually, α-FP is deemed as a tumor maker for various types of cancer, such as testicular cancer, hepatocellular cancer, and so on [15-17]. In healthy human serum, α-FP concentration is low than 25 ng mL^{-1}. However, for patients with liver cancer, α-FP can be detected in a high concentration [18]. Thus, developing an effective and convenient way for testing α-FP in serum is highly desirable in clinical research. Compared to the conventional immunoassay procedures [19-21], electrochemical immunosensors [22] have showed mangy advantages, such as simple instruments, fast analytical time, high sensitivity and specificity, precise current measurements and inexpensive instrumentation.

In this paper, PEDOT, one of the most promising conducting polymers was chosen for the decoration of MWCNTs by a simple interfacial polymerization method according to our previous work [23]. PEDOT wrapping on the MWCNTs provided more anchor centers for obtaining metal nanoparticles with high dispersion. Then, AuNPs were successfully confined on the composite of PEDOT-MWCNTs by chemical reduction method. The incorporation of AuNPs to PEDOT-MWCNTs not only provided binding sites for anti-α-FP immobilization, but also enhanced the electron transfer and amplified the detection signals. In this immune system, the determination of α-FP was achieved by measuring the peak current change of $[Fe(CN)_6]^{3-/4-}$ before and after the immunoreaction. The fabricated immunosensor showed excellent response for α-FP determination and displayed high sensitivity, low detection limit, and good reproducibility. This method was also utilized to monitor α-FP in real sample.

2. EXPERIMENTAL

2.1 Chemicals

Bovine serum albumin (BSA), A-FP and anti-α-FP antibody were obtained from Sigma-Aldrich. The sample of human serum was supplied by a local hospital. 3,4-ethylenedioxythiophene (EDOT) and MWCNTs were purchased from Aladdin Chemistry Co. Ltd. (Shanghai, China). Ferric chloride ($FeCl_3$) was obtained from Shanghai Chemical Company, (Shanghai, China). Chloroform ($CHCl_3$) and $HAuCl_4 \bullet 3H_2O$ were purchased from Sinopharm Chem. Company. (Shanghai, China). 0.1 M Phosphate buffer (pH 7.0) was employed as buffer solution and supporting electrolyte during the whole experiment. Other chemicals were of analytical grade.

2.2 Apparatus

Transmission electron microscope (TEM) was carried out on TEM apparatus (Hitachi, Japan). X-ray diffraction (XRD) patterns were collected on a Rigaku powder diffractometer. Infrared spectra were performed on FTIR apparatus (Perkin Elmer, USA). Electrochemical impedance spectroscopy cyclic voltammetric measurements were performed on a CHI760E electrochemical workstation (Shanghai, China). The three-electrode system was constituted by working electrode (Modified glassy carbon electrode), a platinum wire auxiliary electrode and a saturated calomel reference electrode (SCE).

2.3 Synthesis of PEDOT-MWCNTs and AuNPs/PEDOT-MWCNTs materials

The MWCNTs were purified before use [24]. Typically, MWCNTs (0.5 g) were added into the mixture of HNO_3 and H_2SO_4 (1/3, v/v) under ultrasonication for 6 h. Then, the mixture was centrifuged and washed several times using ultrapure water. The purified MWCNTs were collected and dried over night at 60 °C.

PEDOT-MWCNTs was obtained through interfacial polymerization method. MWCNTs dispersion aqueous (0.5 mg mL^{-1}, 1 mL) was mixed with 1 mL $FeCl_3$ (1 M) and stirred for 25 min. After that, the mixtures were slowly dropped into the $CHCl_3$ solution (2 mL) containing 25 mg mL^{-1} EDOT. An interface was then formed during two layers. After reaction at 50 °C for 24 h, the upper layer mixture was collected by centrifugation, washed several times with ethanol and ultrapure water.

The obtained PEDOT-MWCNTs precipitate was dispersed in 4 mL ultrapure water. 1 mL solution of $HAuCl_4 \cdot 3H_2O$ (5 mM) was mixed with the suspensions of PEDOT-MWCNTs and adequately stirred 15 min. And then, the solution of $NaBH_4$ (0.1 M) was dropped into the mixture while stirring. During the reaction process, Au ions were reduced to AuNPs. The as-prepared AuNPs/PEDOT-MWCNTs material was collected by centrifugation.

2.4 The fabrication of immunosensor

A glassy carbon electrode (GCE, Φ = 3 mm) was carefully polished with 0.05 μm alumina slurry, and then thoroughly cleaned before use. 5 μL of AuNPs/PEDOT-MWCNTs solution was cast on the surface of GCE. And then, it was dried in air.

To immobilize antibody molecules, the prepared AuNPs/PEDOT-MWCNTs/GCE was incubated in the solution of anti-α-FP antibody (200 ng mL^{-1}) for 2 h. After washing, 5 μL BSA solution (1 wt.%) was used to blocked nonspecific binding sites. Subsequently, α-FP solution of different concentration was dropped onto the BSA/anti-α-FP/AuNPs/PEDOT-MWCNTs/GCE and incubated for 50 min. Then the electrode was rinsed thoroughly to remove unbounded α-FP molecules and ready for measurement. Scheme 1 depicted the construction process of the immunosensor.

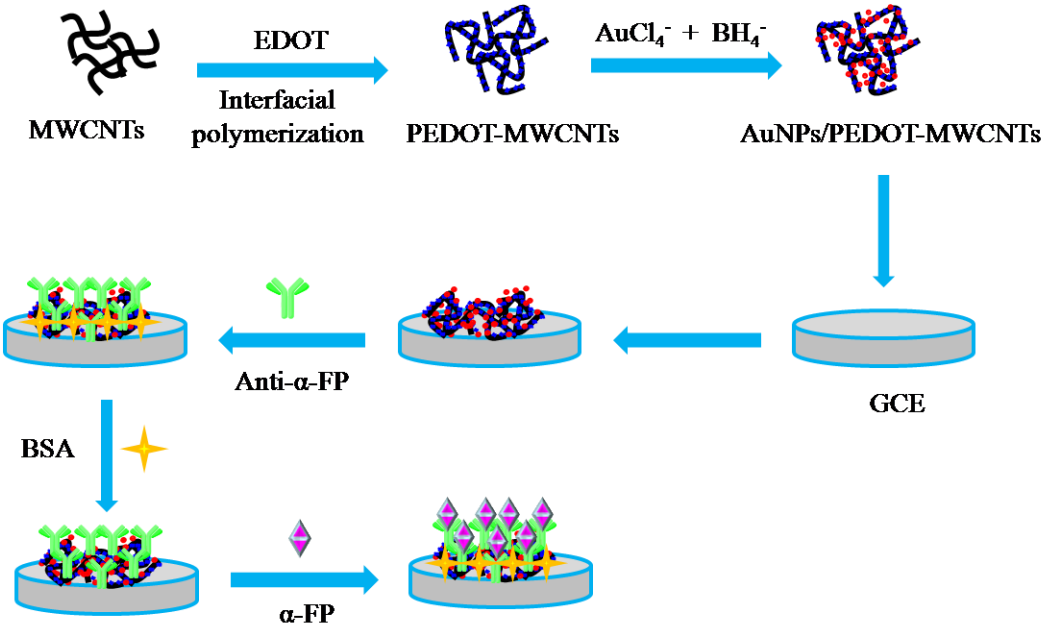

Scheme 1.

2.5 Measurement procedure

Electrochemical experiments were performed in 5 mL phosphate buffer (pH 7.0) with 5 mM $[Fe(CN)_6]^{3-/4-}$. Differential pulse voltammetry (DPV) (potential width: – 0.2 to 0.6 V; pulse period: 0.2 s; amplitude: 50 mV) and cyclic voltammetry (CV) (potential width: – 0.2 to 0.6 V; scan rate: 50 mV s^{-1}) were used to test the electrochemical responses for detecting α-FP. Electrochemical impedance spectroscopy (EIS) was employed to probe the interface of modified electrode. The frequency range is from 0.1 Hz to 100 kHz and the amplitude is 5 mV.

3. RESULTS AND DISCUSSION

3.1 Characterization of AuNPs/PEDOT-MWCNTs nanocomposite

The morphologies of MWCNTs (A), PEDOT-MWCNTs (B) and AuNPs/PEDOT-MWCNTs (C and D) nanocomposites were charactered by TEM. As illustrated in Fig. 1A, the bundles of MWCNTs with smooth surfaces interlocked together [25]. While in Fig. 1B, it demonstrated that uniform PEDOT was distributed on MWCNTs surface. The core-shell nanostructure not only provided considerable specific surface and more binding sites for high mass loading of metal nanoparticles, but also owned the highly conducting capacity. As shown in Fig. 1C and D, small nanoparticles, which represented AuNPs with an average diameter of about (5 ± 2) nm, emerged on the surface of the shell-like structure. The high dispersion AuNPs can increase the immobilized amount of anti-α-FP antibody.

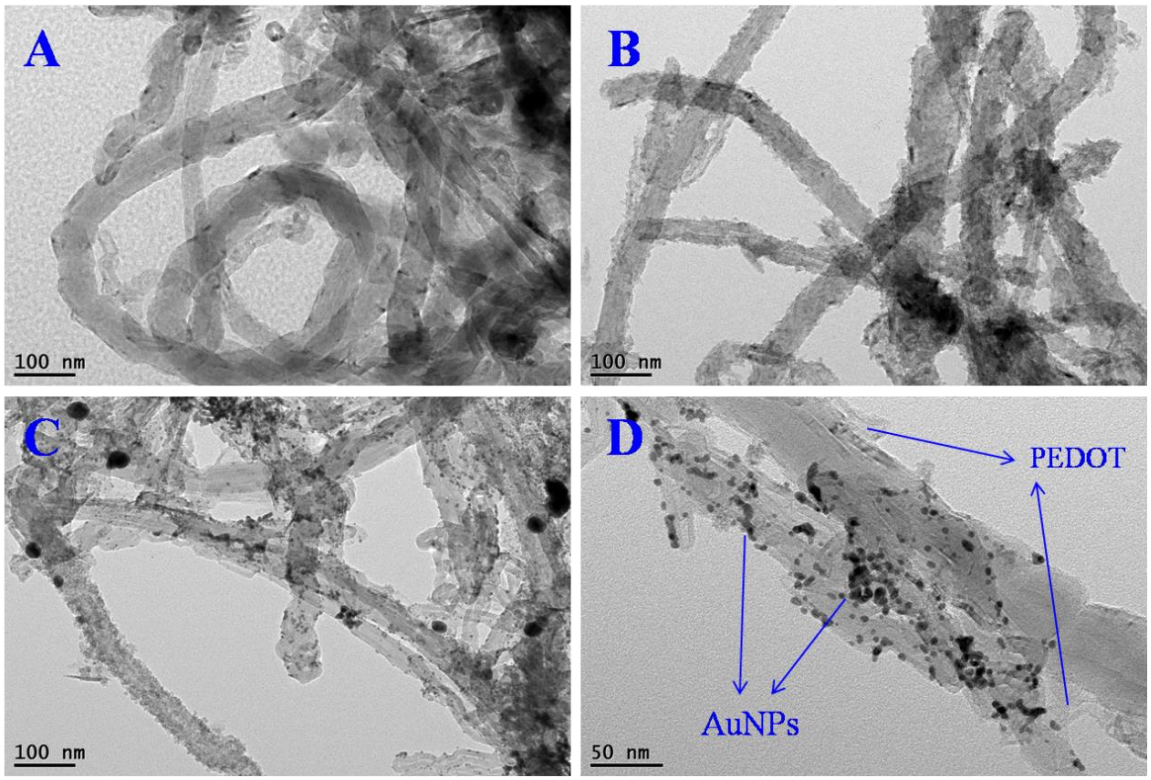

Figure 1. TEM image of MWCNTs (A), PEDOT-MWCNTs (B) and AuNPs/PEDOT-MWCNTs (C, D) at different magnifications.

Fourier transform infrared spectroscopy (FT-IR) was used to study the structures of MWCNTs (a), PEDOT-MWCNTs (b) and AuNPs/PEDOT-MWCNTs (c). In the spectrum of MWCNTs (Fig. 2a), specific absorption peaks of hydroxyl (O–H, 3443 cm^{-1}, 910 cm^{-1}), carbonyl (C=O, 1640 cm^{-1}) and epoxy (C–O–C, 1030 cm^{-1}) groups were observed [26-27], indicating the carboxyl group existed on MWCNTs. For PEDOT-MWCNTs spectrum (b), besides the similar peaks derived from MWCNTs, PEDOT-MWCNTs involved some new peaks at 684, 839, 921 and 984 cm^{-1}, attributing to vibration modes of C–S–C bond on thiophene ring, indicating MWCNTs was functioned by PEDOT film. The spectrum of AuNPs/PEDOT-MWCNTs (c) was similar to PEDOT-MWCNTs except for some small shifts.

The different structures of the MWCNTs (a), PEDOT-MWCNTs (b) and AuNPs/PEDOT-MWCNTs (c) were further studied by XRD (Fig. 2B). For the patterns of MWCNTs, the diffraction peaks at 2θ as 26.12° and 44.39° were ascribed to the (002) and (110) crystalline planes. For PEDOT-MWCNTs (b), a broad diffraction peak appeared at $2\theta \sim 26°$ assigned to the intermolecular spacing of polymer backbone or the (020) reflection [28]. As for AuNPs/PEDOT/GR (c), 2θ of 38.15°, 44.59°, 64.79°, 77.69° and 81.78° that corresponded to the (111), (200), (220), (311) and (222) assigned to the planes of the standard cubic phase of Au, respectively [29].

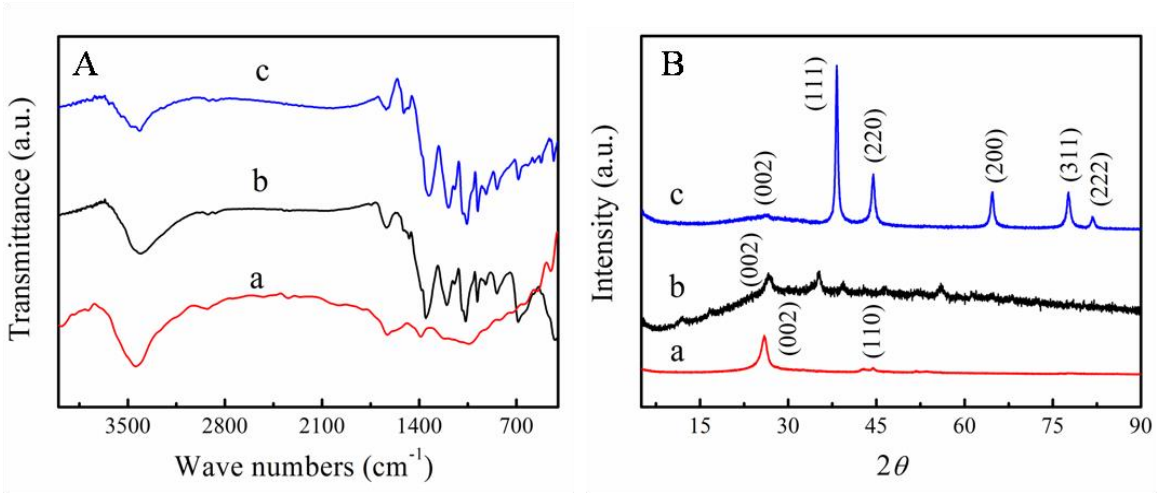

Figure 2. (A) FT-IR and (B) XRD spectroscopy of MWCNTs (a), PEDOT-MWCNTs (b) and AuNPs/PEDOT-MWCNTs (c).

3.2 Electrochemical characteristics of the immunosensor

The electrode interface was studied by CV, which was performed in phosphate buffer (0.1 M, pH 7.0) containing 5 mM $K_3[Fe(CN)_6]/K_4[Fe(CN)_6]$ (1:1) (Fig. 3A). The peak current increased when bare GCE (curve a) was modified with PEDOT-MWCNTs (curve b). After AuNPs were imported into PEDOT-MWCNTs, the current (curve c) was further increased. This is because that AuNPs have good electric conductivity and act as conducting wires to accelerate electron transfer [30,31]. In contrast, peak currents gradually decreased after anti-α-FP and BSA (curve d and curve e) were modified on the electrode. Finally, after the immunosensor was incubated with the insulating α-FP, the current decreased again (curve f)

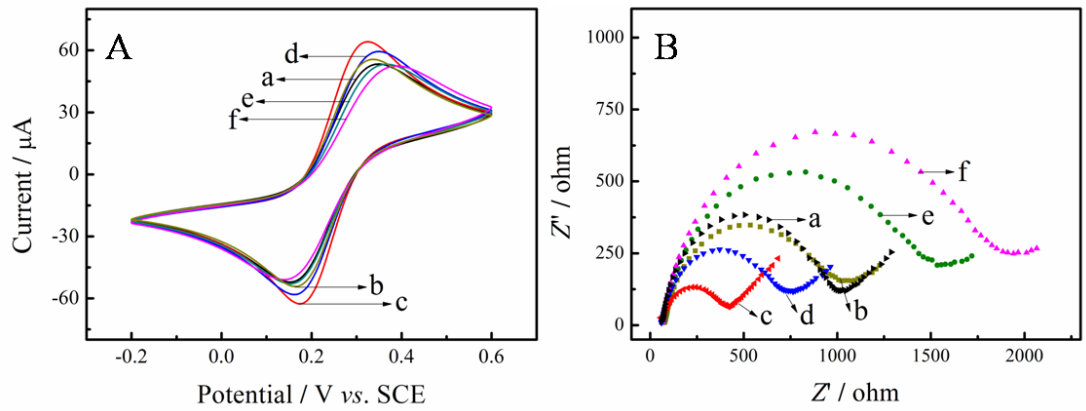

Figure 3. Cyclic voltammograms (A) and electrochemical impedance spectroscopy (B) of the different electrodes: bare GCE (a), PEDOT-MWCNTs/GCE (b), AuNPs/PEDOT-MWCNTs/GCE (c), anti-α-FP/AuNPs/PEDOT-MWCNTs/GCE (d), BSA/anti-α-FP/AuNPs/PEDOT-MWCNTs/GCE (e) and α-FP/BSA/anti-α-FP/AuNPs/PEDOT-MWCNTs/GCE (f).

Electrochemical impedance spectroscopy (EIS) was also used to investigate the assembly process. As shown in Fig. 3B, bare GCE (curve a) showed low electron transfer resistance (Ret). After PEDOT-MWCNTs composite was decorated on the GCE surface, the R_{et} decreased, which was ascribed to the excellent electric conductivity of PEDOT and MWCNTs. With the deposition of AuNPs into PEDOT-MWCNTs composites, the R_{et} further decreased (curve c). However, when anti-α-FP (curve d) and BSA (curve e) were modified onto the surface of AuNPs/PEDOT-MWCNTs/GCE, the resistances increased step by step, which might be due to the fact that the insulating proteins of anti-α-FP and BSA hindered the electron transfer. As the α-FP was incubated was with immunosensor (curve f), the R_{et} was further increased.

3.3 Optimization of experimental conditions

The effect of pH on the immunosensor was studied from 5.5 to 8.0 with 0.5 ng mL^{-1} α-FP (Fig. 4a). The current change increased with the increase of pH from 5.5 to 7.0. While, decrease of current change can be observed with further increase of pH. Thus pH 7.0 was fixed for further experiments.

The effect of temperature on the immunoreaction was examined from 4 to 40 °C. From Fig. 4b, maximum current change can be observed with a temperature around 30 °C. As a result, the incubation temperature of 30 °C was selected for the detection.

Incubation time effect on the current change was also studied. As shown in Fig. 4c, ΔI increased with the increasing incubation time and then started to level off at 50 min. Therefore, the 50 min of incubation time was used in this study.

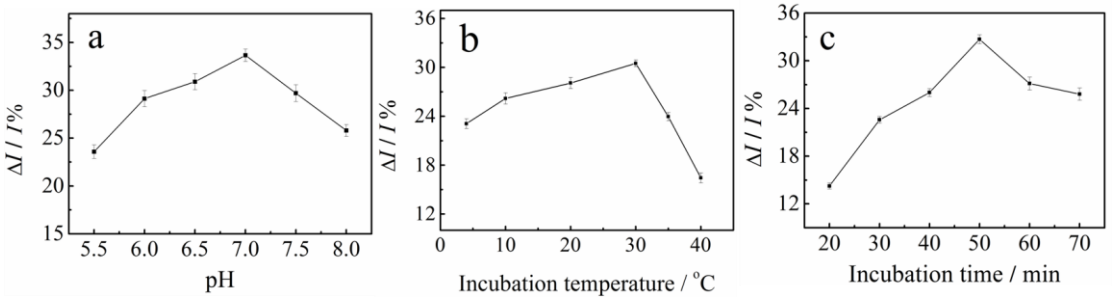

Figure 4. Influence of the pH of the phosphate buffer (a), incubation temperature (b) and incubation time (c) on the current responses of the developed immunosensor.

Under the optimized parameter, the fabricated method was employed for detecting a series of different concentrations of α-FP. Fig. 5 displays the typical DPV responses to α-FP with various concentrations using the immunosensor. The DPV current signal decreased in response to increasing concentrations of α-FP. The current responses exhibited a linear relationship with the logarithmic values of α-FP concentration from 0.0005 to 10 ng mL^{-1} (the inset graph in Fig. 5). The linear regression equation was ΔI (μA) = 47.6951 + 12.2659 × log C [α-FP] (ng mL^{-1}, R^2 = 0.9927, n = 3). The detection limit was estimated to be 0.0002 ng mL^{-1} (S/N= 3).

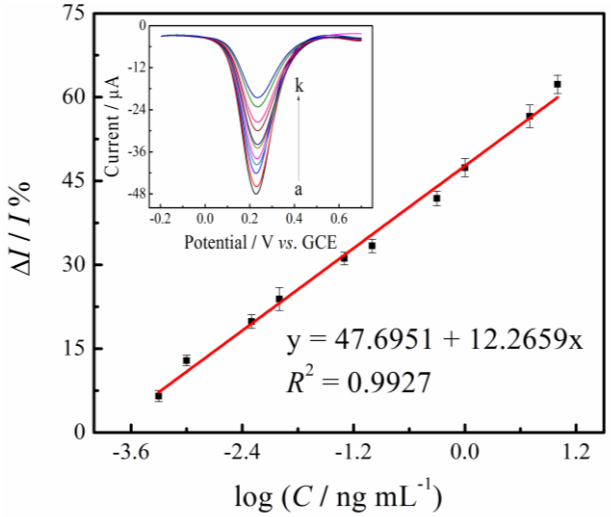

Figure 5. Differential pulse voltammetry of the immunosensor for the detection of different concentrations of α-FP (a–k: 0, 0.0005, 0.001, 0.005, 0.01, 0.05, 0.1, 0.5, 1, 5 and 10 ng mL^{-1}). The inset shows the calibration curve based on the change of the DPV peak currents versus the logarithm of the concentrations.

In addition, the analytical performance of the proposed method was compared with that of some previously α-FP immunosensors (Table 1). The present sensor had lower detection limit [31-36], which might be ascribed to the fact that the large amount of AuNPs could provide more active surface area to absorb anti-α-FP.

Table 1. Analytical performance of electrochemical immunosensors for detection of α-FP.

Immunosensors	Linear range (ng mL^{-1})	Detection limit (ng mL^{-1})	References
CS/CdS/TiO_2/ITO electrode	0.05-20	0.02	[32]
Au/SnO_2/graphene/GCE	0.02-50	0.01	[33]
Pd-rGO/GCE	0.01-12	0.005	[34]
Au/PB/MWCNT/GCE	0.01-300	0.003	[35]
nano-Au/nano-SiO_2/PB/Au elecrode	0.05-200	0.02	[36]
[a]Au-PtNPs/NiHCFNPs/Au-PtNPs/GCE	0.06-13 and 13-200	0.017	[37]
AuNPs/PEDOT/MWCNTs/GCE	0.0005-10	0.0002	This work

[a]NiHCFNPs: nickel hexacyanoferrate nanoparticles.

3.4 Selectivity, reproducibility and stability of the immunosensor

Carcinoembryonic antigen (CEA), human immunoglobulin G (IgG), BSA, ascorbic acid and glucose have been chosen to study the selectivity of the fabricated immunosensor. The peak currents for the immunosensor incubated in α-FP (0.5 ng mL^{-1}) without or with 5 ng mL^{-1} interfering substance were tested (Fig. 6A). These results suggested the immunosensor displayed good specificity for the determination of α-FP.

The reproducibility was estimated by determining 0.5 ng mL^{-1} α-FP with five different electrodes. The relative standard deviation (RSD) of the measurements was 5.36% for the five electrodes, demonstrating excellent reproducibility of the fabrication protocol. The stability of the immunosensor was also studied by successive cycle scan. A 6.94% decrease of the initial response can be seen after 30 successive CV measurements in phosphate buffer (pH 7.0) (Fig. 6B). These demonstrated that the stability of immunosensor was good.

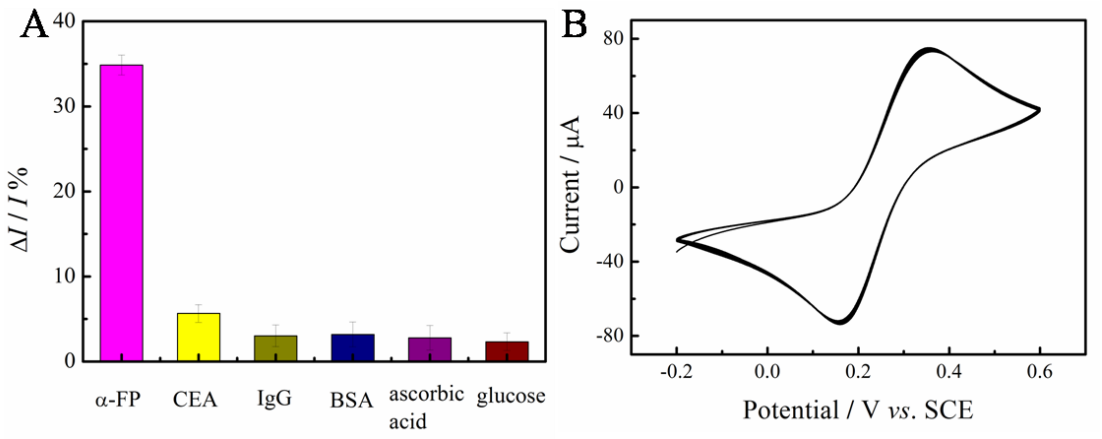

Figure 6. (A) Comparison of the response of the immunosensor to 0.5 ng mL^{-1} α-FP, 5 ng mL^{-1} CEA, IgG, BSA, ascorbic acid and glucose. (B) Successive 30 CV cycles of the immunosensor in phosphate buffer containing 0.1 M KCl (pH 7.0).

3.5 Real sample analysis

To investigate the practicability of the immunosensor, recovery experiments were used for detecting α-FP using standard addition methods in serum samples. As can be seen from Table 2, the RSD was in the range from 1.46% to 5.83%. The recovery was in the range from 94.93% to 104.63%, suggesting that the method is available for α-FP determination in human serum.

Table 2. Detection of α-FP added in human serum (n = 3) with the proposed method.

Sample	Added of α-FP (ng mL^{-1})	Found (ng mL^{-1})	RSD (%)	Recovery (%)
1	0.1	0.083 0.094 0.112	1.46	96.33
2	0.5	0.442 0.476 0.506	3.14	94.93
3	1	0.980 1.065 1.094	5.83	104.63
4	5	4.849 4.937 4.852	4.96	97.58

4. CONCLUSIONS

In summary, a new electrochemical immunosensor for α-FP determination was constructed using the AuNPs/PEDOT-MWCNTs nanocomposite material. PEDOT-MWCNTs nanocomposites were made by a liquid-liquid interface method, and then a number of AuNPs about (5 ± 2) nm were uniformly attached on the PEDOT-MWCNTs surface as the immunosensor platform. Benefited from the excellent electron transfer ability of AuNPs/PEDOT-MWCNTs nanocomposites, the method displayed wide linear range and low detection limit.

ACKNOWLEDGEMENTS
We are grateful to the National Natural Science Foundation of China (grant number: 21665010, 51302117, 51303073, 51463008), Ganpo Outstanding Talents 555 projects (2013), the Natural Science Foundation of Jiangxi Province (grant number: 20151BAB203018, 20142BAB206028 and 20142BAB216029), Postdoctoral Science Foundation of China (2014M551857 and 2015T80688), Postdoctoral Science Foundation of Jiangxi Province (2014KY14) and State Key Laboratory of Chemical Biosensing & Chemometrics (2015010) for their financial support of this work.

References

1. J. Liu, J. Wang, T. Wang, D. Li, F. Xi, J. Wang, *Biosens. Bioelectron.*, 65 (2015) 281
2. I. Ojeda, B. Garcinu o, M. Moreno–Guzmán, *Anal. Chem.*, 86 (2014) 7749
3. S. Iijima, *Nature*, 354 (1991) 56
4. L. Liu, W. Ma, Z. Zhang, *Small*, 7 (2011) 1504
5. C. Shi, C. Deng, X. Zhang, P. Yang, *ACS Appl. Mat. Interfaces*, 5 (2013) 7770
6. Y.S. Gao, L.P. Wu, K.X. Zhang, J.K. Xu, L.M. Lu, X.F. Zhu, *Chin. Chem. Lett.*, 26 (2015) 613
7. A.S. Emami Meibodi, S. Haghjoo, *Synthetic Met.*, 194 (2014) 1
8. H.C. Choi, M. Shim, S. Bangsaruntip, H.J. Dai, *J. Am. Chem. Soc.*, 124 (2002) 9058
9. H. Kim, N.J. Jeong, S.J. Lee, K.S. Song. *Korean J. Chem. Eng.*, 25 (2008) 443
10. Y.Y. Mu, H.P. Liang, J.S. Hu, L. Jiang, L.J. Wan, *J. Phys. Chem., B* 109 (2005) 22212
11. M.H. Yang, Y.H. Yang, Y.L. Liu, G.L. Shen, R.Q. Yu, *Biosens. Bioelectron.*, 21 (2006) 1125
12. S. Samanman, A. Numnuam, W. Limbut, P. Kanatharana, P. Thavarungkul. *Anal. Chim. Acta*, 853 (2015) 521
13. Y. Cheng, P.K. Shen, S.P. Jiang, *Int. J. Hydrogen Energy*, 39 (2014) 20662
14. M. Zhang, L. Su, L.Q. Mao, *Carbon*, 44(2006) 276
15. X. Huang, X. Deng, D. Wu, *Anal. Methods*, 4 (2012) 3575
16. G.K. Parshetti, F. Lin, R. Doong, *Sensor Actuat. B*, 186 (2013) 34
17. J. Guo, X. Han, J. Wang, J. Zhao, Z. Guo, Y. Zhang, *Anal. Biochem.*, 491 (2015) 58
18. H. Li, Y. Zhang, Q. Wei, H. Ma, D. Wu, Y. Li, *Biosens. Bioelectron.*, 53 (2014) 305
19. Z. Fu, C. Hao, X. Fei, H. Ju, *J. Immunol. Meth.*, 312 (2006) 61
20. L. Belanger, C. Sylvestre, D. Dufour, *Clin. Chim. Acta*, 48 (1973) 15
21. T. Kawabata, M. Watanabe, K. Nakamura, *Anal. Chem.*, 77 (2005) 5579
22. H.B. Noh, M.A. Rahman, J.E. Yang, Y.B. Shim, *Biosens. Bioelectron.*, 26 (2011) 4429
23. G. Qi, Z. Wu, H. Wang, *J. Mater. Chem. C*, 1 (2013) 7102
24. J. Zhang, H. Zou, Q. Qing, Y. Yang, Q. Li, *J. Phys. Chem. B*, 107 (2003) 3712
25. S. Yang, J. Li, D. Shao, J. Hu, X. Wang, *J. Hazard. Mater.*, 166 (2009)109
26. X.Y. Dong, X.N. Mi, L. Zhang, T.M. Liang, J.J. Xu, *Biosens. Bioelectron.*, 38 (2012) 337
27. L. Ji, Z. Guo, T. Yan, H. Ma, B. Du, Y. Li, Q. Wei, *Biosens. Bioelectron.*, 68 (2015) 757

28. J.W. Choi, M.G. Han, S.Y. Kim, S.G. Oh, *Synthetic Met.*, 141 (2004) 293
29. S.V. Selvaganesh, J. Mathiyarasu, K.L.N. Phani, *Nanoscale Res. Lett.*, 2 (2007) 546
30. B. Kavosi, R. Hallaj, H. Teymourian, *Biosens. Bioelectron.*, 59 (2014) 389
31. Y. Zhuo, P.X. Yuan, R. Yuan, Y.Q. Chai, C.L. Hong, *Biomaterials*., 29 (2008) 1501
32. X. Yang, J. Li, J. Fu, *Anal. Methods*, 7 (2015) 1328
33. J. Liu, G. Lin, C. Xiao, Y. Xue, A. Yang, H. Ren, W. Lu, *Biosens. Bioelectron.*, 71 (2015) 82
34. T.T. Qi, J.F. Liao, Y.S. Li, J.R. Peng, W.T. Li, B.Y. Chu, *Biosens. Bioelectron.*, 61 (2014) 245
35. Jiang W, Yuan R, Chai YQ, Yin B, *Anal. Biochem.*, 407 (2010) 65
36. X. Huang, X. Deng, D. Wu, *Anal. Methods*, 4 (2014) 3575
37. Q. Zhu, R. Yuan, Y. Chai, J. Han, Y. Li, N. Liao, *Analyst*, 138 (2013) 620